Proceedings of IMECE04
2004 ASME International Mechanical Engineering Congress and Exposition
November 13-20, 2004, Anaheim, California USA

IMECE2004-60931

DIRECTED ASSEMBLY OF METAL OXIDE NANOBELTS WITH MICROSYSTEMS INTO INTEGRATED NANOSENSORS

Choongho Yu
Dept. of Mechanical Engineering
Center for Nano and Molecular Science and Technology
The University of Texas at Austin
Austin, TX 78712

Qing Hao
Dept. of Mechanical Engineering
Center for Nano and Molecular Science and Technology
The University of Texas at Austin
Austin, TX 78712

Li Shi
Dept. of Mechanical Engineering
Center for Nano and Molecular Science and Technology
The University of Texas at Austin
Austin, TX 78712
Email: lishi@mail.utexas.edu

Dae-Jin Kang
Dept. of Mechatronics Engineering
Korea Polytechnic University
Shiheung, Kyunggi, Korea

Xiangyang Kong
School of Materials Science and Engineering
Georgia Institute of Technology
Atlanta, GA 30332

Z. L. Wang
School of Materials Science and Engineering
Georgia Institute of Technology
Atlanta, GA 30332

ABSTRACT

Single-crystalline tin dioxide (SnO_2) nanobelts have been assembled with microfabricated suspended heaters as low-power, sensitive gas sensors. With less than 4 mW power consumption of the micro-heater, the nanobelt can be heated up to 500^{o}C. The electrical conductance of the heated nanobelt was found to be highly stable and sensitive to toxic and inflammable gas species including dimethyl methyl phosphonate (DMMP), nitrogen dioxide (NO_2), and ethanol. The experiment is a step towards the large scale integration of nanomaterials with microsystems, and such integration via a directed assembly approach can potentially enable the fabrication of low-power, sensitive, and selective integrated nanosensor systems.

INTRODUCTION

Metal oxide sensors are commonly used to monitor a variety of toxic and inflammable gases in an air pollution monitoring system, food industry, medical diagnosis equipment, and gas-leak alarms. The sensing mechanism is based on a surface oxidation or reduction process that changes the concentration of oxygen vacancies in the metal oxide and thus alters its electrical conductance [1,2]. Because only the surface layer is affected by the reaction, the sensitivity of a metal oxide sensor increases for decreasing thickness, motivating the development of thin film metal oxide sensors with the use of microelectromechanical system (MEMS) technologies [3]. A key component of the MEMS sensor is a thermally isolated membrane structure with a built-in thin film resistor that is Joule-heated up to 500 ^{o}C. The high temperature enhances the oxidation or reduction process and improves the sensitivity. However, when the thickness of a metal oxide film deposited by a physical or chemical vapor deposition method is reduced below 100 nm to achieve the ultimate sensitivity, the film often consists of a high density of pinholes and defects that lead to unstable electrical properties. Additionally, grain boundaries in the film are responsible for degradation and poisoning of the sensor. These problems have prevented the reduction of the film thickness, limiting the sensitivity of thin film metal oxide sensors to a few parts per million (ppm) of gas species.

Recently, belt-like metal oxide nanostructures have been synthesized [4,5]. These metal oxide nanobelts are single crystalline. Because the nanobelt can be as thin as 10 nm, almost the entire thickness is affected by the oxidation or reduction process with environmental gas species. In an earlier work [6], tin dioxide (SnO_2) nanobelts have been tested for gas sensing. When the nanobelt was heated using an external heater, it showed a sub-ppm level sensitivity for detecting nitrogen dioxide (NO_2) gas. Moreover, the absence of grain boundaries in these single crystalline structures allows for long-term stability and reliability, the lack of which

has prevented the wide application of polycrystalline thin film metal oxide sensors.

A major challenge for the development of sensor technologies based on "bottom-up" synthesized nanostructures, e.g. carbon nanotubes [7,8], semiconductor nanowires [9], and metal oxide nanobelts, is the large-scale manufacturing of well-organized nanostructure sensor arrays with the complex functionality comparable to that of MEMS sensors. Examples of such functionality include thermal and flow controls that can be integrated with MEMS sensors. In this paper, we report the assembly of SnO_2 nanobelts with MEMS heater devices into low-power, highly sensitive detectors of gas species. The MEMS device provides localized thermal control for the nanobelt, eliminating the need for an external heater that consumes much more power. Moreover, the experiment represents a step towards the large-scale integration of nanomaterials with microsystems, and the integration can potentially enable the fabrication of low-power, sensitive, and selective nano-sensor systems.

EXPERIMENT

The MEMS device was originally designed for measuring the thermal and thermoelectric properties of one-dimensional nanostructures [10]. As shown in Fig. 1, it consists of two adjacent silicon nitride (SiN_x) membranes supported by long SiN_x beams. A serpentine platinum (Pt) resistance thermometer (RT) is patterned on each membrane. The RT can be Joule heated to increase the operating temperature of the sensor as well as to monitor the sensor temperature. Two separate parallel Pt electrodes are patterned on the two membranes, forming an electrode pair for trapping the nanobelt.

Nanobelts can be trapped on the Pt electrode pair using three different approaches. In the first one, a solution containing the nanobelts is dropped on a wafer that contains a large number of densely-packed membrane structures. After the solution was spun on the wafer, nanobelts were often adsorbed between the two Pt electrodes that were 2-5 μm apart and few nanobelts were deposited between the long SiN_x beams that were approximately 12 μm apart from each other. Alternatively, nanobelts can be placed on MEMS devices with the use of a micromanipulation method based on the atomic force microscope (AFM) [11]. To increase the assembly yield, we have investigated an electric field-directed assembly method. In this method, the two Pt electrodes in the MEMS device are connected to an ac voltage source. As a solution containing the nanobelts is dispersed on the surface of the MEMS array, the frequency of the ac field can be adjusted to generate an attractive force on the nanobelts that are polarized in the electric field. This phenomenon is called positive dielectrophoresis [12], where a polarizable particle in a non-uniform ac electric field is attracted to regions of high field strength. The attractive or positive dielectrophoretic force can be used to align and trap a nanobelt onto the two Pt electrodes. We found that the suitable frequency and root-mean-square (rms) amplitude of the ac voltage are about 1 MHz and 5 V, respectively, for trapping the nanobelt. Usually several nanobelts are stacked between two electrodes, but this does not hamper the performance of the sensor. Similar methods have been reported for trapping nanowires [13,14] and nanotubes [15] with a yield approaching 100%.

RESULTS

Figure 1 shows a single SnO_2 nanobelt trapped on the two Pt electrodes of the MEMS device. The sensor temperature can be raised up to 500°C with the use of Joule heating in the Pt RTs. Because of the large thermal resistance in the long and low-thermal conductivity SiN_x beams, the membrane is thermally isolated from the substrate. Hence, the device only consumed 3.8 mW for raising the membrane temperature to 500°C, as shown in Fig. 2.

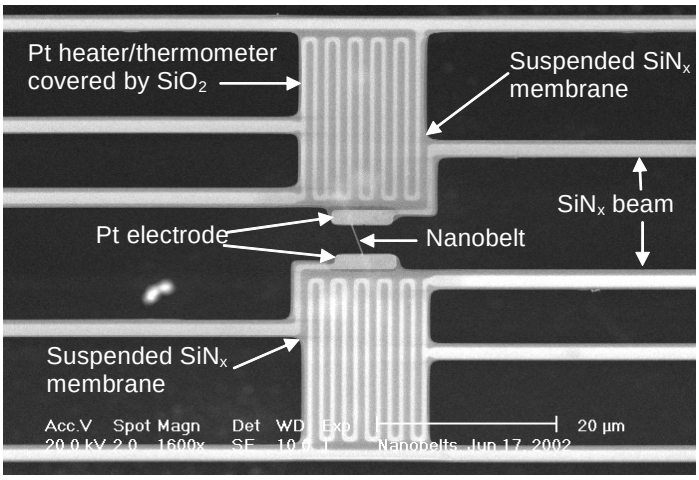

Fig. 1 Scanning electron micrograph (SEM) of a SnO_2 nanobelt assembled on two Pt electrodes of a MEMS device that consists of two suspended SiN_x membranes each supported by five long SiN_x beams. A Pt serpentine is patterned on each membrane.

The temperature rise shown in Fig. 2 was measured with the use of the Pt RT. In brief, the voltage drop (V) in the RT was measured as the dc heating current (I) was slowly ramped up. The differential resistance of the RT heater is calculated as $R = dV/dI$. For a slow voltage ramp rate, it can be shown that the temperature rise in the heating membrane is

$$\Delta T(I) = \frac{\Delta R(I)}{3R'}; \qquad (1)$$

$$\Delta R(I) = R(I) - R(I=0),\ R' = \frac{dR(I=0)}{dT}$$

where R' is the temperature dependence of the resistance and was measured separately in a cryostat.

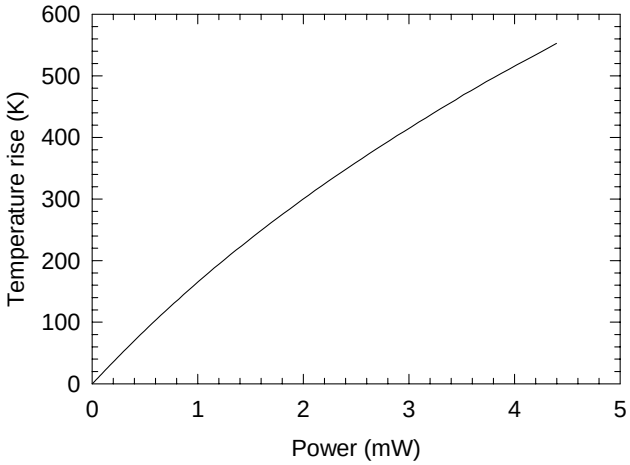

Fig. 2 Temperature rise of the suspended membrane as a function of power consumption of the Pt heater line.

To test the as-assembled nanobelt sensor, the sensor was mounted in a small flow-through chamber. For NO_2 or ethanol, a cylinder containing the gas species balanced with air was connected to a mixing chamber through a flow meter, as shown in Fig. 3a. To vary the concentration of the gas species, room air was purged into the mixing chamber through a flow meter. The sensor chamber was connected to the mixing chamber in order to deliver the gas mixture. For dimethyl methyl phosphonate (DMMP), a permeation tube containing liquid phase of DMMP was used. To evaporate DMMP, the permeation tube was heated in a U-shape stainless steel tubing. Room air was purged to the tubing in order to deliver DMMP vapor to a mixing tee, as shown in Fig.3b. The concentration of the gas species can be calculated as C=K×P/F, where C, F, P, and K are concentration in ppm by volume, diluent flow rate in cc/min, permeation rate in ng/min, and molar constant (=24.46/molecular weight), respectively [16]. An air pump was connected to the mixing tee in order to vary the concentration of DMMP. A DC current was supplied to the Pt RT on the membrane to raise the temperature of the nanobelt. With a constant voltage applied to the nanobelt, the current through the nanobelt was recorded when the chamber was purged with a gas species and room air, repeatedly.

Figure 4 shows the sensor response to 78 and 53 ppb DMMP balanced with air when the device was Joule-heated to 500 ^{o}C. The dotted lines in the figure represent the gas concentrations that flowed to the sample chamber. Figure 5 shows the sensor response to 0.2, 0.5, 0.9, 1.7, and 10 ppm NO_2 balanced with air when the nanobelt was Joule-heated to 200 ^{o}C. As the NO_2 gas was introduced to the chamber, the current dropped immediately and recovered quickly after NO_2 gas was replaced by room air. The reduction in current increased with the NO_2 gas concentration, being about 45% change in current at 10 ppm concentration. More importantly, it does not show sensor-poisoning effects because of the absence of grain boundaries in the nanobelt.

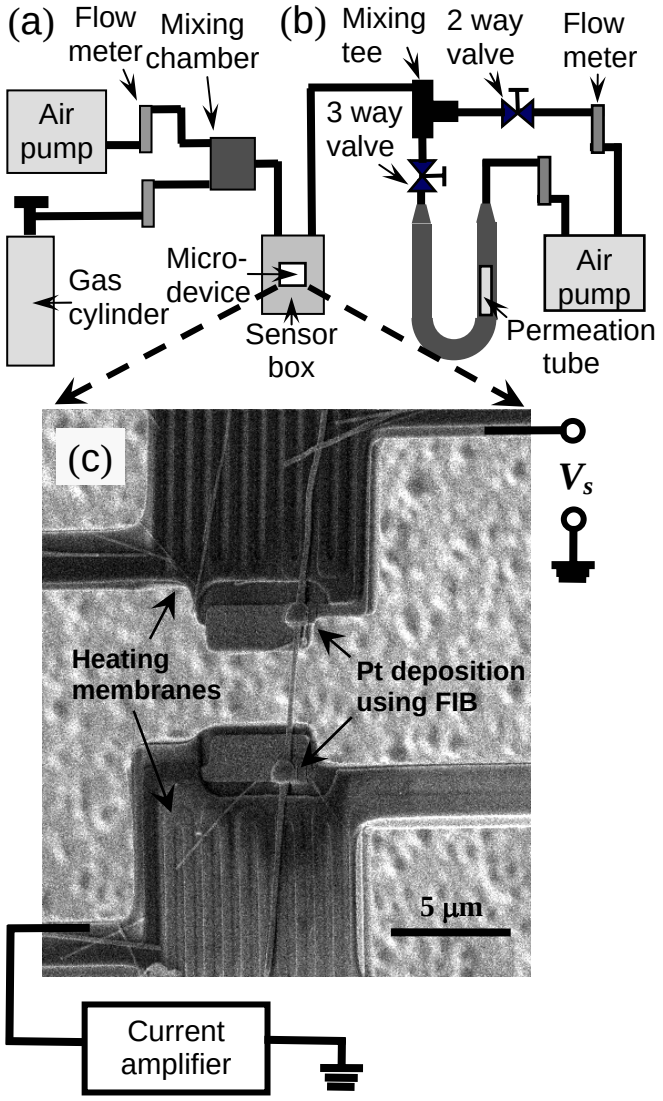

Fig. 3 Experimental setup to test the nanobelt sensor for (a) NO_2 and Ethanol gas species, (b) DMMP gas species. (c) SEM of a SnO_2 nanobelt assembled on two Pt electrodes of the membranes. To enhance electrical conductivity and prevent sensor poisoning effect, Pt was deposited on the two contacts using focused ion beam (FIB) technique.

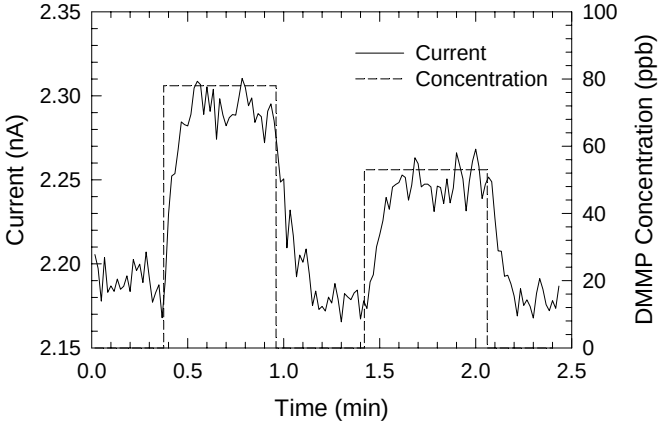

Fig. 4 Response of the as-assembled nanobelt sensor to 78 and 53 ppb DMMP balanced with air when the nanobelt temperature was 500 ^{o}C. The voltage applied to the nanobelt was 1.5 V.

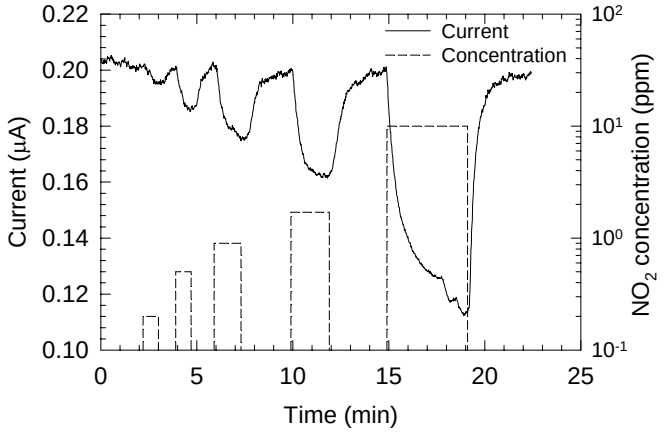

Fig. 5 Response of the as-assembled nanobelt-MEMS sensor to 0.2, 0.5, 0.9, 1.7, and 10 ppm NO_2 balanced with air when the nanobelt temperature was 200 ^{o}C. The voltage applied to the nanobelt was 2 V.

Figure 6 shows the sensor response to 125, 83, 250, and 23 ppm ethanol balanced with air when the device was Joule-heated to 330 ^{o}C. While the NO_2 gas depletes electrons by forming NO^{2-} on the sensor surface, OH- group in the ethanol gas desorbs oxygen ions from the nanobelt and thereby enhances electrical conductance, leading to an increase in current soon after the ethanol gas was introduced to the chamber.

As shown in Fig. 4, 5, and 6, the sensor response was highly repeatable and fast compared with sensors based on carbon nanotube films [17] or a bunch of nanobelts [6]. Note that the excellent recovery could only be achieved with Pt deposition on the contacts. Without Pt deposition, the conductance did not recover fully or quickly due to contact poisoning.

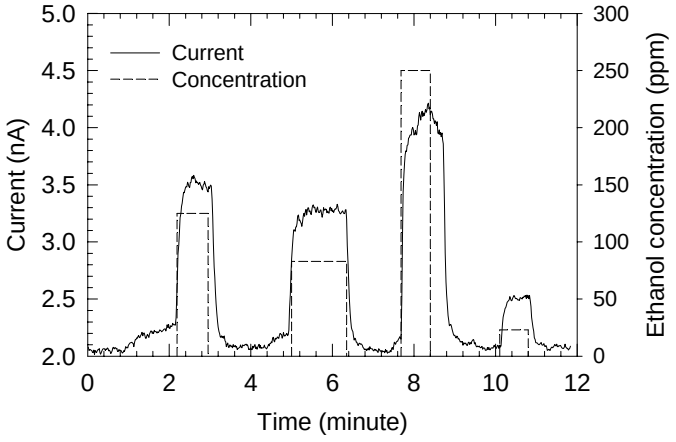

Fig. 6 Response of the as-assembled nanobelt-MEMS sensor to 125, 83, 250, and 23 ppm ethanol balanced with air when the nanobelt temperature was 330 ^{o}C. The voltage applied to the nanobelt was 1.0 V.

SUMMARY

These experiments show that low-power, miniaturized gas sensors can be fabricated by assembling metal oxide nanobelts with MEMS devices. The sensitivity of the as-assembled sensor can be further enhanced by functionalizing the nanobelts with different catalytic additives [3, 18]. The selectivity of metal oxide sensors can be obtained using a pattern recognition approach, where an array of different nanobelt sensors generates a distinct response pattern for a gas species or mixture. With the use of the electric field-directed assembly method or a directed growth method, moreover, it is feasible to fabricate selective gas sensor arrays consisting of functionalized metal oxide nanobelts assembled into a MEMS platform that consists of a micro chromatography column [19] and pre-concentrator [20] for gas separation and pre-concentration. This directed assembly approach can thus enable one to combine nanomaterials synthesis with MEMS fabrication for the large-scale manufacturing of integrated nano-sensor systems.

ACKNOWLEDGMENTS

This work was supported by NSF grant number CTS-0239179. We thank D. Li and A. Majumdar for helpful discussions.

REFERENCES

[1] Gardner, J. W., 1994, *(Bio)chemical Microsensors, in Microsensors: Principles and Applications*, John Wiley and Sons, West Sussex, UK, p 224.

[2] Morrison, S. R., *Chemical Sensors*, 1994, *Semiconductor Sensors*, John Wiley and Sons, New York, NY.

[3] Kovacs, G. T. A., *Micromachined Transducers Sourcebook*, McGraw-Hill, Boston, 1998.

[4] Pan, Z. W., Dai, Z. R., and Wang, Z. L., 2001, "Nanobelts of Semiconducting Oxides," Science, **291**, pp. 1947-1949.

[5] Dai, Z. R., Pan, Z. W., and Wang, Z. L., 2003**,** "Novel Nanostructures of Functional Oxides Synthesized by Thermal Evaporation" Advanced Functional Materials, **13**, pp. 9-13.

[6] Comini, E., Faglia, G.., Sberveglieri, G.., Pan, Z. W., and Wang, Z. L., 2002**,** "Stable and Highly Sensitive Gas Sensors Based on Semiconducting Oxide Nanobelts" Appl. Phys. Lett., **81**, pp. 1869-1871.

[7] Collins, P.G., Bradley, K., Ishigami, M., and Zettl A., 2000, "Extreme Oxygen Sensitivity of Electrical Properties of Carbon Nanotubes," Science, **287**, pp. 1801-1804.

[8] Shim, M., Wong, N., Kam, S., Chen, R. J., Li, Y., and Dai, H., 2002, "Functionalization of Carbon Nanotubes for Biocompatibility and Biomolecular Recognition," Nano Lett., **2 (4)**, pp. 285-288.

[9] Cui, Y.; Wei, Q.; Park, H.; Lieber, C. M., 2001, "Nanowire Nanosensors for Highly Sensitive and Selective Detection of Biological and Chemical Species" Science, **293**, pp. 1289-1292.

[10] Shi, L., Li, D., Yu, C., Jang, W., Yao, Z., Kim, P., and Majumdar, A., 2003, "Measuring Thermal and Thermoelectric Properties of One-Dimensional Nanostructures Using a Microfabricated Device," Journal of Heat Transfer, **125**, pp. 881-888.

[11] Hughes, W. and Wang, Z. L., 2003, "Nanobelts as Nanocantilevers," Appl. Phys. Lett., **82**, pp. 2886-2888.

[12] Pohl, H. A. , 1978, *Dielectrophoresis*, Cambridge University Press, London, UK.

[13] Chen, X. Q., Saito, T., Yamada, H., and Matsushige, K., 2001, "Aligning Single-Wall Carbon Nanotubes with an Alternating-Current Electric Field," Appl. Phys. Lett., **78**, pp. 3714.

[14] Smith, P. A., Nordquist, C. D., Jackson, T. N., Mayera, T. S., Martin, B. R., Mbindyo, J., and Mallouk, T. E., 2000, "Electric-Field Assisted Assembly and Alignment of Metallic Nanowires," Appl. Phys. Lett., **77**, pp. 1399–1401.

[15] Duan, X., Huang, Y., Cui, Y., Wang, J., and Lieber, C. M., 2001, "Indium Phosphide Nanowires as Building Blocks for Nanoscale Electronic and Optoelectronic Devices," Nature, **409**, pp. 66-69.

[16] Product manual, Dynacal permeation device, VICI Metronics, Inc.

[17] Novak, J. P., Snow, E. S., Houser, E. J., Park, D., Stepnowski, J. L., and McGill, R. A., 2003, "Nerve Agent Detection Using Networks of Single-walled Carbon Nanotubes," Appl. Phys. Lett., **83(19)**, pp. 4026-4028.

[18] Oh, S. W., Kim, Y. H., Yoo, D. J., Oh, S. M., and Park, S. J., 1993, "Sensing Behaviour of Semiconducting Metal Oxides for the Detection of Organophosphorus Compounds," Sensors and Actuators B, **13-14**, pp.400-403.

[19] Noh, H. S., Hesketh, P. J., and Frye-Mason, G. C., 2002, "Parylene Gas Chromatographic Column for Rapid Thermal Cycling," J. Microelectromechanical Systems, **11**, pp. 718-725.

[20] Tian, W.-C., Pang, S.W., Lu, C.-J., and Zellers, E. T., 2003, "Microfabricated Preconcentrator-Focuser for a Microscale Gas Chromatograph," J. Microelectromechanical Systems, **12**, pp. 264-272.